Inorganic Chemistry

pubs.acs.org/IC Article

Synthesis, Characterization, and Biological Evaluation of Iron(III)-N-Heterocyclic Carbene Complexes as Photosensitizers for Photodynamic Therapy and Chemotherapeutics against Cancer

Lei Zhou,[#] Giulia Salluce,[#] Pierre Mesdom, Marta Redrado, Lisa Gourdon-Grünewaldt, Samia Hidalgo, Olivier Blacque, Philippe Arnoux, Céline Frochot, Kevin Cariou,* and Gilles Gasser*



Cite This: Inorg. Chem. 2025, 64, 17058-17065



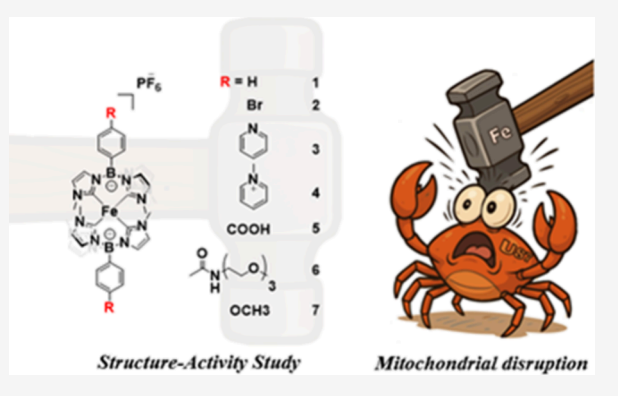
ACCESS I

III Metrics & More

Article Recommendations

Supporting Information

ABSTRACT: Photodynamic therapy (PDT) is a promising strategy for cancer treatment, yet the reliance on rare, expensive, and potentially toxic heavy metals limits the practical application of many current photosensitizers. In this study, we synthesized and evaluated a series of iron(III)-*N*-heterocyclic carbene (Fe(III)-NHC) complexes (1–7) bearing diverse substituents to explore their potential as cost-effective alternatives for cancer therapy. While none of the complexes exhibited significant singlet oxygen generation under light excitation, several (particularly complexes 1, 2, 3, and 7) showed strong cytotoxicity toward cancer cells even in the absence of photodynamic activation. Structure—activity analysis revealed that hydrophobic or moderately electron-donating groups enhanced cellular uptake and bioactivity, while polar or bulky substituents reduced efficacy of cellular uptake, as



confirmed by ICP-MS and confocal fluorescence microscopy. Further biological studies suggested that the cytotoxic effects of these compounds may stem from mitochondrial damage, potentially caused by disruption of mitochondrial membrane potential through iron-mediated redox processes. These findings highlight the promise of Fe(III)-NHC complexes as potential chemotherapeutic agents and underscore the importance of rational ligand design in modulating their biological activity.

INTRODUCTION

Photodynamic therapy (PDT) has emerged as a promising approach for cancer treatment due to its precise spatiotemporal selectivity, minimal invasiveness, and ability to selectively destroy tumor tissues with reduced damage to surrounding healthy cells.^{1,2} It serves as a powerful complement to conventional therapies like surgery, chemotherapy, and radiotherapy. Among various PDT agents, metal-based photosensitizers (PSs) have attracted significant attention owing to their superior photophysical and photochemical properties, including high water solubility, excellent photostability, efficient reactive oxygen species (ROS) generation, and favorable (photo)chemical stability. 1,3-6 These features grant them considerable advantages in therapeutic performance and clinical potential. Heavy metal complexes such as those of ${\rm Ir}({\rm III}),^{7-10} {\rm Ru}({\rm II}),^{11-13}$ and ${\rm Os}({\rm II})^{14-16}$ have shown exceptional PDT performance and have been extensively studied. However, these heavy metals are relatively scarce and expensive, which limits their large-scale application and raises sustainability concerns. In contrast, first-row transition metals (e.g., iron, copper, manganese, cobalt) are abundant, costeffective, and environmentally friendly, making them highly attractive candidates as next-generation PSs. Therefore, the development of first-row transition metal-based PSs represents

a more promising and forward-looking strategy for advancing PDT in both research and clinical settings. In pursuit of this challenging goal, significant efforts have been devoted to designing complexes based on first-row transition metals. 17,18 Among these, iron has attracted particular attention. For example, Chakravarty and co-workers developed several phototoxic Fe(III)-based complexes to induce cell death upon light excitation, utilizing a dipyrido[3,2-d:2',3'-f]quinoxaline or a dipicolylamine moiety as effective PS scaffolds. 19-24 Inspired by the traditional Ru(II) polypyridine complexes,²⁵ our group has developed several Fe(II) polypyridine complexes analogues.^{26,27} However, these iron complexes exhibited low emission intensity, poor singlet oxygen quantum yields, and limited phototoxic effects. This is primarily attributed to the inherently low emission efficiency and ultrashort excited-state lifetimes of Fe(II) complexes,

Received: July 11, 2025 Revised: August 5, 2025 Accepted: August 8, 2025 Published: August 14, 2025





Scheme 1. Synthesis Route for the Fe(III)-NHC Complexes 1-7

Figure 1. Molecular structure of complex 6 (all H atoms are omitted for clarity). Displacement ellipsoids are drawn at the 30% probability level.

C11

B1

N₅

C18

C17

C25

C24

caused by low-lying metal-centered (MC) states that facilitate rapid deactivation of the excited charge-transfer (CT) states. Recent studies, however, have demonstrated that incorporating strongly σ -donating N-heterocyclic carbene (NHC) ligands can elevate the energy levels of MC states relative to CT states, thereby prolonging the excited-state

C15

C16

C19

C22

lifetimes and enhancing the photophysical properties of iron complexes. 30,31 Notably, a heteroleptic Fe(II) complex bearing tripyridine and NHC ligands has been reported as an efficient PS for light-driven water reduction. In addition, the recent discovery of an NHC Fe(III) complex with exceptional photophysical properties by Wärnmark and co-workers

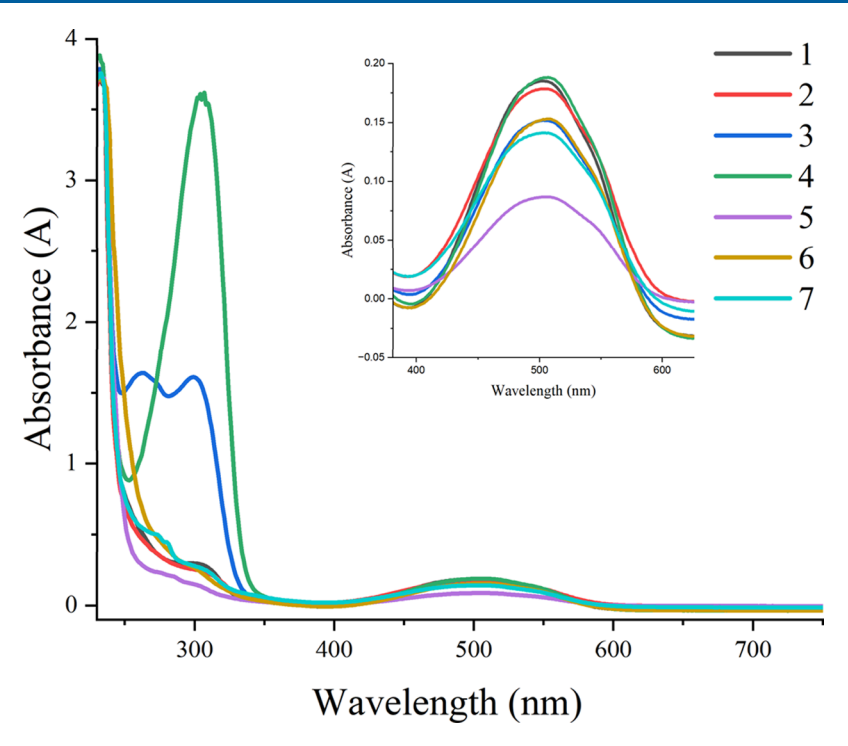


Figure 2. UV-vis spectra of the Fe(III)-NHC complexes 1-7 in CH₃CN (50 μ M).

renewed hope for the development of iron-based PSs.³² This Fe(III)-NHC complex was found to feature a charge-transfer excited state with a 2 ns lifetime and a 2.1% emission quantum yield under air-saturated acetonitrile. These remarkable improvements in excited-state lifetime, photostability, and visible-light emission compared to traditional iron complexes highlight its potential for biomedical and photochemical applications.

Inspired by the works described above, herein, we synthesized Fe(III)-NHC complexes 1–7 bearing different substituents, which were subsequently characterized and biologically evaluated (Scheme 1). The *N*-methylpyridinium and the PEG chain substituents were introduced in complexes 4 and 6 to improve their water solubility. All complexes display visible-light absorption around 500 nm, making them attractive for light-triggered applications. Despite their inability to produce singlet oxygen for photodynamic tumor cell killing, several of these compounds (1, 2, 3, 7) demonstrate significant cytotoxicity against cancer cells, indicating their promise as potential chemotherapeutic candidates.^{33,34}

■ RESULTS AND DISCUSSION

Synthesis and Characterization. The metal complexes synthesized in this work are illustrated in Scheme 1. The syntheses of compounds 1, 2, 5, and 7 have been previously reported in the literature. ^{32,35} Different NHC precursors L1, L2, L3 were synthesized using phenyltrimethylsilane, 4-bromophenyltrimethylsilane and 4-methoxyphenyltrimethylsilane as starting materials, respectively. The Fe(III) complexes 1, 2 and 7 were synthesized by the reaction of the imidazolium carbene precursors and FeCl₂ in the presence of *t*-BuOK (1 M in THF) under nitrogen atmosphere. Modification of complex 2 with a pyridine unit by a Suzuki cross-coupling yielded complex 3, which was subsequently methylated to afford the *N*-methylpyridinium complex 4. The improved aqueous solubility of complex 4 is attributed to the increased polarity

and ionic character of the substituent. Additionally, the introduction of a highly water-soluble PEG group in complex 5 yielded complex 6. Detailed procedures and characterizations are provided in the Supporting Information. The structures of all complexes were confirmed by ¹H and ¹³C NMR spectroscopy (Figure S1-S19) and high-resolution mass spectrometry (Figure S20-S26). Dark red single crystals of complexes 3, 4, and 6 were successfully obtained by slow diffusion of diethyl ether into acetonitrile. Single-crystal X-ray diffraction studies were carried out. Crystal data, structure refinement parameters and molecular structures are provided in the Supporting Information (Figure 1, Figure S27-S28 and Table S1-S3). The coordination of the iron center with the bis-tridentate NHC ligand led to the formation of complexes with an octahedral geometry. Neither electron-donating nor electron-withdrawing substituents, including pyridine, pyridinium salts, or PEG chains, exert a significant influence on the Fe-C bond lengths (2.00-1.96 Å) or the C-Fe-C bite angles (87.3-86.7°). The asymmetric unit of complex 3 consists of two independent half cations of $C_{46}H_{46}B_2FeN_{14}^{}$, a $PF_6^{}$ anion, and three acetonitrile molecules. The anion is fully disordered over two sets of positions with site-occupancy factors of 0.201(2) and 0.799(2). One of the three solvent molecules of acetonitrile is also disordered over two sets of positions with site-occupancy factors of 0.452(5) and 0.548(5). Similarity restraints were applied to the P-F, C-N and C-C bond lengths in the disordered parts, while the corresponding atoms were restrained to have similar atomic displacement parameters. The crystal structure of complex 4 was refined as a nonmerohedral 2-component twin. The crystals were very flat red plates and it was not possible to get an untwinned piece. The cations lie on centers of inversion. The anions lie on general positions and on centers of inversion. The former ones are disordered over two sets of positions (except the central P atoms) with site-occupancy factors of 0.506(5) and 0.494(5). There are no strong hydrogen bonds in the crystal structure.

The predominant features of the crystal packing are $C-H\cdots F$ and $C-H\cdots \pi$ intermolecular close contacts. The crystal structure of complex 6 has been solved and refined successfully with no unusual features. The cations lie on centers of inversion while the anions lie on general position.

Photophysical Properties. Afterwards, we tested the photophysical properties of the prepared metal complexes 1-7to evaluate the prospects of their applications for PDT and chemotherapy. The UV-vis spectra of complexes 1-7 show an absorbance from 240 to 700 nm (Figure 2). All seven complexes exhibit similar absorption profiles. In the 400-600 nm region, a broad band around 500 nm is observed for all compounds, which can be assigned to a second ligand-to-metal charge transfer (2LMCT) transition as it was described by Wärnmark et al.³² The different substituents at the paraposition of the benzene ring have minimal influence on the absorption characteristics in this region. All complexes also display strong absorption bands in the UV region (<350 nm), which are attributed to intraligand $\pi - \pi^*$ transitions. Notably, complexes 3 and 4, bearing a pyridine and an Nmethylpyridinium substituent, respectively, exhibit significantly enhanced absorbance in the UV region, likely due to the stronger electron-withdrawing nature of these groups. For further investigation of the photophysical properties, complexes 1-7 were excited at 500 nm and their emission was measured in CH₃CN. All complexes exhibit a broad emission band from 550 to 850 nm, which maximum is at 645 nm (Figure S29). Notably, the complexes were found to be only weakly emissive, with fluorescence quantum yields of approximately 4% and 5% in CH₃CN. Additionally, their excited-state lifetimes were around 1.6 ns at room temperature, under an oxygen concentration of approximately 21% of saturation. No singlet oxygen emission was observed for these iron complexes in CH₃CN (Table 1), which is consistent with the biological results.

Table 1. Photophysical Properties of the Iron Complexes in CH_3CN^a

compounds	fluorescence quantum yield (%)	fluorescence lifetime (ns)	singlet oxygen quantum yield	
Ru(bpy) ₃	7.7		0.77	
1	4.0	1.7	0.00	
2	5.0	1.6	0.00	
3	4.0	1.6	0.00	
4	4.0	1.5	0.00	
5	4.0	1.6	0.00	
6	5.0	1.6	0.00	
7	4.0	1.6	0.00	

"Tris(2,2'-bipyridyl) Ru(II) in acetonitrile was chosen as a standard for both fluorescence and singlet oxygen quantum yield determination. The lifetimes were measured at room temperature and a concentration of oxygen in the samples of around 21% of the saturation.

(Photo)chemical Stability. To ensure that the synthesized complexes maintain their structural integrity and functional properties during use, we systematically investigated the stability of complexes 1–7 in a commonly used organic solvent and biological medium. The stability was evaluated in CH₃CN and DMEM supplemented with 10% FBS and 1% antibiotics by UV–vis spectroscopy. Complexes 1–7 were dissolved in the test solvent and stored at 37 °C. The

absorption spectrum of each complex was recorded from 250 to 750 nm after each time interval (0, 2, 6, 24, 48, and 72 h). The solubility of complex 1 in DMEM decreases significantly over time; however, its absorption bands remain unchanged. This series of experiments suggests that all complexes are stable in CH₃CN and biological medium (Figure S30 and S31). Subsequently, we investigated the photostability of the compounds in the biological medium. The stability was evaluated before illumination, immediately after illumination at 540 nm for 40 min, and at 2, 6, and 24 h post-light irradiation. Importantly, no significant changes in the absorption spectra of complexes 1–7 were observed in biological medium after illumination (Figure S32).

Cytotoxicity. To evaluate the potential activity of the iron complexes as PSs, a fluorometric viability assay was performed on glioblastoma cells (U87) and noncancerous retinal pigmentary epithelial cells (RPE-1), with and without illuminating the cells at 540 nm, a wavelength corresponding to a major absorption peak for all synthesized compounds. For this purpose, cells were incubated with different concentrations of complexes 1-7 diluted in complete culture medium up to 100 μ M. After 4 h, the compound solutions were replaced with fresh complete culture medium. Protoporphyrin IX (PpIX) was used as a positive control for photoactivation, while the clinically approved chemotherapeutic agent cisplatin was tested under the same conditions (without light excitation) for comparison. This screening showed that complexes 4, 5, and 6 are nontoxic or present fairly low toxicity for both cell lines at the tested concentrations. None of the compounds shows a remarkable photoactivation upon illumination, but, surprisingly, complexes 1, 2, 3, and 7 are highly cytotoxic after a short incubation (4 h) – unlike cisplatin that needs longer treatment time³⁶ – even in the absence of light excitation, presenting IC_{50} values between 1.87 and 2.87 μM in U87 cells, and between 2.85 and 5.06 μM in RPE-1 cells. Upon light excitation, a slight increase in cytotoxicity is observed, particularly in cancer cells (see Table 2). Even though the photoactivation of the cytotoxic complexes is not as effective as the one of the control compound PpIX, they show higher selectivity toward cancer cells (Figure S33).

Overall, although the iron complexes do not display strong photoinduced effects, the pronounced dark cytotoxicity and selective activity of complexes 1, 2, 3, and 7 in U87 cells suggest their potential as promising anticancer agents deserving further exploration.

Cellular Uptake and Localization Studies. The cellular uptake of the complexes was then investigated in U87 cells by determining the amount of boron inside the cells using inductively coupled plasma mass spectrometry (ICP-MS). The evaluation of boron amount (contained in the ligand) was preferred to iron's one because the presence of iron in biological environments could affect the results. ICP-MS analysis of cells incubated for 4 h with 1 μ M of complexes 1–7 show that the cellular uptake of the less active compounds namely 4, 5, and 6 - is extremely low, comparable to the untreated control, while complexes 1, 2, 3, and 7 - those showing the highest cytotoxicity - accumulate in cells to a greater extent (Figure 3a). These results suggest that the different substituents of the synthesized compounds play an important role in the intracellular internalization, which is crucial to observe a biological effect.

To obtain further insight into the cellular uptake and subcellular localization, confocal fluorescence microscopy

Table 2. IC₅₀ Values in the Dark and upon Irradiation (Light) at 540 nm (9 J⋅cm⁻²) on Glioblastoma (U87) and Noncancerous Retinal Pigmentary Epithelial (RPE-1) Cells^a

Compound	Cell line	IC_{50} dark (μ M)	IC_{50} light (μ M)	PI
1	U87	1.87 ± 0.24	0.93 ± 0.16	2.00
	RPE-1	4.30 ± 0.22	3.05 ± 0.21	1.41
2	U87	1.47 ± 0.08	0.24 ± 0.11	6.05
	RPE-1	2.85 ± 0.29	2.71 ± 0.67	1.05
3	U87	2.36 ± 0.32	0.40 ± 0.11	5.93
	RPE-1	6.51 ± 0.19	4.48 ± 0.28	1.45
4	U87	50.98 ± 7.56	19.40 ± 5.10	2.63
	RPE-1	>100	>100	n.d.b
5	U87	>100	>100	n.d.b
	RPE-1	>100	>100	n.d.b
6	U87	>100	58.46 ± 6.57	n.d.b
	RPE-1	>100	>100	n.d.b
7	U87	2.87 ± 0.00	2.01 ± 0.25	1.43
	RPE-1	5.06 ± 0.48	4.94 ± 0.97	1.02
PpIX	U87	71.33 ± 7.89	1.25 ± 0.03	57.2
	RPE-1	>100	0.39 ± 0.04	n.d.b
Cisplatin	U87	14.82 ± 2.12	n.d. ^a	n.d.b
	RPE-1	>100	n.d.ª	n.d.b
Ligand L1	U87	>100	n.d.ª	n.d.b
	RPE-1	>100	n.d.ª	n.d.b

[&]quot;Average of three independent measurements. PI = phototoxicity index (IC_{50} dark/ IC_{50} light); n.d. = not done; n.d. = not determinable.

studies were performed on cells incubated for 4 h with compound concentrations corresponding to their IC₂₅. Although all compounds display low quantum yields, intracellular fluorescence is clearly detectable for complexes 1 and 7, confirming the efficient uptake observed by ICP-MS. Complexes 2 and 3 show weaker intracellular fluorescence, in agreement with their slightly lower internalization level detected by ICP-MS. The less active compounds show barely

detectable or undetectable intracellular fluorescence corroborating the hypothesis of their lower biological activity related to the inability to internalize inside the cells (Figure 3b). Regarding the subcellular localization, the detectable compounds do not colocalize with any particular organelle, including nucleus, mitochondria, endoplasmic reticulum, or endolysosomal compartment, as shown by the absence of colocalization with the relative markers (Figure S34), but rather exhibit heterogeneous distribution inside the cytoplasm. Interestingly, the mitochondria of cells treated with the most active compounds present compromised morphology, as the organelle marker MitoTracker do not show the typical mitochondrial staining pattern (Figure S34b). Following the observation of this disruption, we conducted further studies to estimate the impact of our compounds on mitochondrial respiration.

Mitochondrial Respiration Studies. Mitochondria are organelles responsible for producing adenosine triphosphate (ATP) through oxidative phosphorylation. In addition to the production of energy, they play key roles in various metabolic pathways, the maintenance of ROS homeostasis, and the regulation of apoptosis and programmed cell death.^{37,38} In cancer cells, mitochondrial function is crucial and contributes significantly to sustaining cell viability.³⁹ The Seahorse XF Analyzer was used to investigate the effect of the iron complexes on the mitochondrial respiration through the Mito Stress Test, performed following the Agilent protocol. 40 U87 cells were incubated for 4 h with the compounds at a concentration of 1 µM. After degassing the culture medium for 1 h in a non-CO₂ incubator, the cells were treated with sequential injections of specific inhibitors of the electron transport chain. First, oligomycin was added to inhibit the ATP synthase, then carbonyl cyanide 4-(trifluoromethoxy) phenylhydrazone (FCCP) was then added as an uncoupling agent that induces maximal oxygen consumption rate (OCR), finally a combination of rotenone/antimycin A was injected to block the electron transport chain to stop the mitochondrial O₂

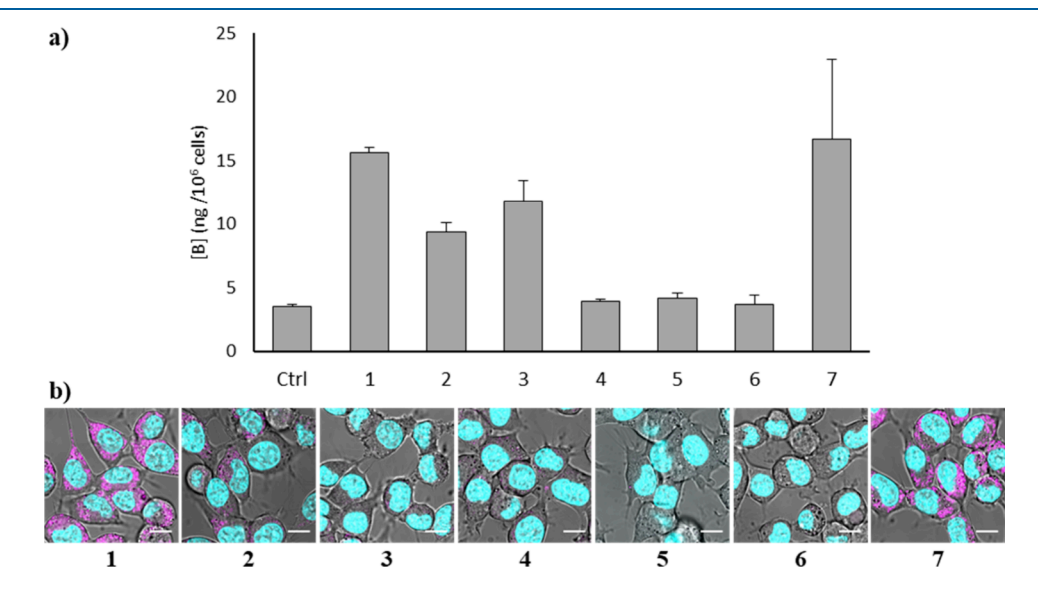


Figure 3. Cellular uptake and localization studies. (a) Whole cell accumulation in U87 cells after 4 h incubation of 1 μ M of complexes 1–7 (and untreated cells as a control) assessed by Boron-11 quantification using high-resolution ICP-MS. The represented bars are the mean of three replicates with related standard deviations. (b) Intracellular distribution of complexes 1–7 by confocal microscopy. Live U87 cells were imaged following incubation with the compounds (magenta) at concentrations corresponding to their IC₂₅ for 4 h and then with Hoechst 33342 (cyan) to stain the nuclei. Scale bars are 10 μ m.

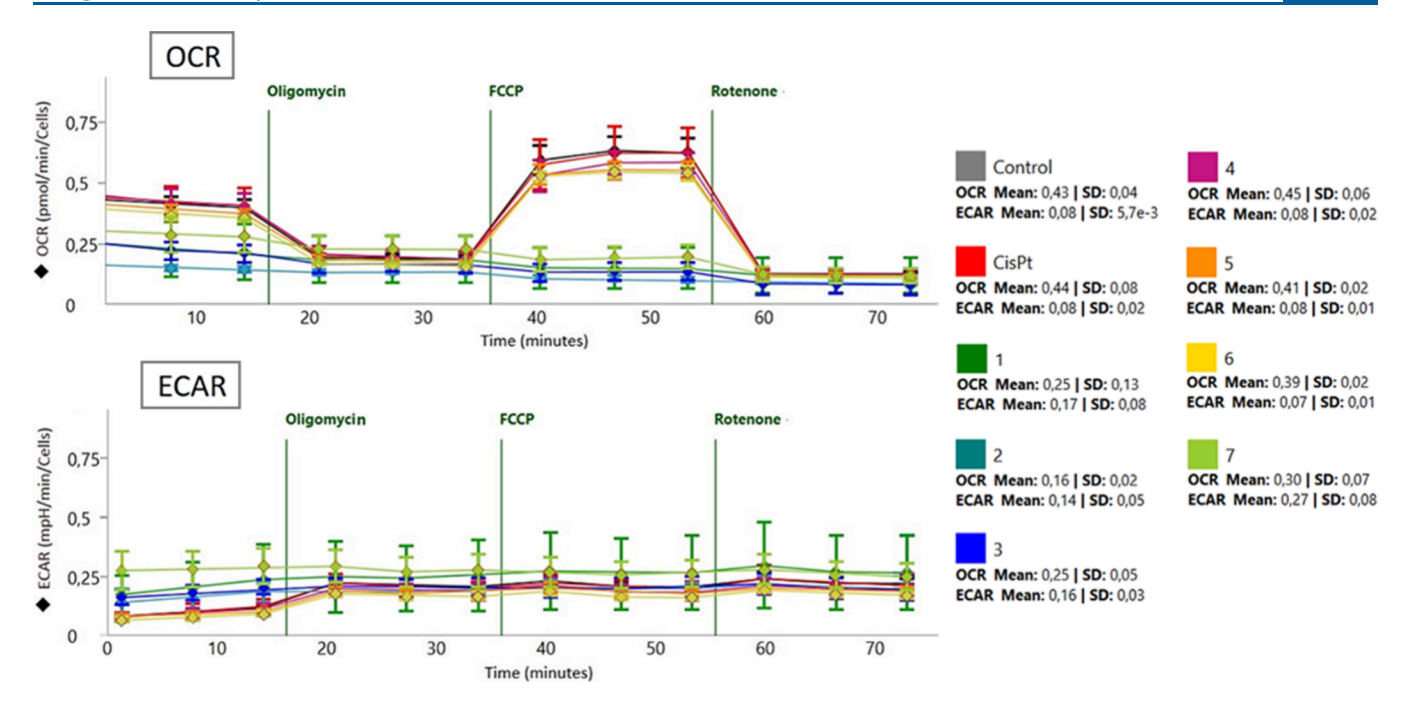


Figure 4. OCR (top) and ECAR (bottom) profiles obtained by performing the Mito Stress Test in U87 cells after 4 h of treatment. Oligomycin, FCCP, and rotenone together with antimycin A were sequentially added by the Seahorse XF analyzer. The represented points are the mean of three replicates with related standard deviations. The color code is pictured on the right, including the mean values of OCR and ECAR for each condition, with related standard deviations.

consumption. The results show that, in cells treated with the most active complexes (1, 2, 3, and 7), ATP synthase is not affected by the addition of oligomycin and the maximum OCR reached after the addition of FCCP is very low, indicating a severe impairment of mitochondrial respiration (Figure 4). This is probably due to a permeabilization of the mitochondrial membrane, as suggested by the confocal microscopy images displaying an irregular mitochondrial staining in cells treated with complexes 1, 2, 3, and 7 (Figure S34b). This hypothesis is also supported by the higher extracellular acidification rate (ECAR) presented by cells treated with the four active compounds, indicating a switch to the glycolytic metabolism for ATP production following a severe mitochondrial damage (Figure 4). The less active complexes (4, 5, and 6) display OCR and ECAR profiles similar to those of the controls, i.e. untreated cells and cells treated with cisplatin, which is known not to significantly affect mitochondrial respiration at low concentrations and short exposure times (Figure 4).³⁷

CONCLUSIONS

In summary, we synthesized a series of Fe(III)-NHC complexes 1–7 with different substitution groups. After physical and biological evaluation, we found that they were not effective in generating singlet oxygen to kill cancer cells. However, they demonstrated excellent toxicity against tumor cells. The potential of the synthesized complexes to be used as chemotherapeutic agents has a direct relationship with their structure. The most cytotoxic complexes (1, 2, 3, and 7) share common structural features, such as hydrophobic or moderately electron-donating substituents (e.g., aryl, arylbromide, pyridyl, or methoxy groups), which are associated with enhanced cellular uptake, as evidenced by our ICP-MS and confocal microscopy analyses. In contrast, the less active complexes (4, 5, and 6) bear highly polar or bulky

substituents—including carboxylic acids, quaternary ammonium groups, or polyethylene glycol chains—which likely reduce their membrane permeability and overall bioavailability. These observations suggest that the attentive selection of functional groups is crucial to achieve the desired biological activity. Furthermore, the presented studies suggest that the cytotoxic character of these compounds involves mitochondrial damage. This might be due to the redox properties of iron complexes, which lead them to interfere with and disrupt the mitochondrial membrane potential. Overall, this study demonstrates that such iron-based organometallic complexes are promising compounds for further studies as anticancer agents.

■ EXPERIMENTAL SECTION

Materials and Methods. All the reagents were purchased from commercial sources and used without further purification. The solvents were dried according to standard procedures. The compounds were prepared as depicted in Scheme 1 and the detailed synthetic procedures and characterizations are given in the Supporting Information.

ASSOCIATED CONTENT

Data Availability Statement

All data associated with this study are present in the paper or the Supporting Information.

Supporting Information

The Supporting Information is available free of charge at https://pubs.acs.org/doi/10.1021/acs.inorgchem.5c03185.

Experimental details: chemical synthesis, biological experiments, methods and procedures, instrumentation and characterization; additional data: NMR spectra, stability studies, selected crystal data and structure refinement parameters (PDF)

Accession Codes

Deposition Numbers 2471023—2471025 contain the supplementary crystallographic data for this paper. These data can be obtained free of charge via the joint Cambridge Crystallographic Data Centre (CCDC) and Fachinformationszentrum Karlsruhe Access Structures service.

AUTHOR INFORMATION

Corresponding Authors

Kevin Cariou — Chimie ParisTech, PSL University, CNRS, Institute of Chemistry for Life and Health Sciences, Laboratory for Inorganic Chemical Biology, Paris 75005, France; Email: kevin.cariou@chimieparistech.psl.eu

Gilles Gasser — Chimie Paris Tech, PSL University, CNRS, Institute of Chemistry for Life and Health Sciences, Laboratory for Inorganic Chemical Biology, Paris 75005, France; orcid.org/0000-0002-4244-5097; Email: gilles.gasser@chimieparistech.psl.eu

Authors

Lei Zhou – Chimie ParisTech, PSL University, CNRS, Institute of Chemistry for Life and Health Sciences, Laboratory for Inorganic Chemical Biology, Paris 75005, France

Giulia Salluce — Chimie ParisTech, PSL University, CNRS, Institute of Chemistry for Life and Health Sciences, Laboratory for Inorganic Chemical Biology, Paris 75005, France

Pierre Mesdom — Chimie ParisTech, PSL University, CNRS, Institute of Chemistry for Life and Health Sciences, Laboratory for Inorganic Chemical Biology, Paris 75005, France

Marta Redrado — Chimie ParisTech, PSL University, CNRS, Institute of Chemistry for Life and Health Sciences, Laboratory for Inorganic Chemical Biology, Paris 75005, France; orcid.org/0000-0001-5201-0874

Lisa Gourdon-Grünewaldt — Chimie ParisTech, PSL University, CNRS, Institute of Chemistry for Life and Health Sciences, Laboratory for Inorganic Chemical Biology, Paris 75005, France; orcid.org/0000-0003-0932-7838

Samia Hidalgo – Institut de Physique du Globe de Paris, Biogéochimie à l'Anthropocène des Eléments et Contaminants Emergents, Paris 75005, France

Olivier Blacque – Department of Chemistry, University of Zurich, Zurich 8057, Switzerland

Philippe Arnoux — Université de Lorraine, CNRS, LRGP, Nancy F-54000, France; orcid.org/0000-0002-6834-9597

Céline Frochot – Université de Lorraine, CNRS, LRGP, Nancy F-54000, France; orcid.org/0000-0002-7659-3864

Complete contact information is available at: https://pubs.acs.org/10.1021/acs.inorgchem.5c03185

Author Contributions

[#]L.Z. and G.S. contributed equally to the work.

Notes

The authors declare no competing financial interest.

ACKNOWLEDGMENTS

L.Z. thanks the China Scholarship Council for financial support. G.S. thanks Xunta de Galicia for her postdoctoral

contract (ED481B-2023-123). M.R. thanks the Fondation pour la Recherche Médicale (FRM) for their financial support (SPF202309017545).

ABBREVIATIONS

CT, charge-transfer; DMEM, Dulbecco's modified Eagle medium; ECAR, extracellular acidification rate; FBS, fetal bovine serum; FCCP, carbonyl cyanide-4-(trifluoromethoxy)-phenylhydrazone; IC₅₀, half maximal inhibitory concentration; ICP-MS, inductively coupled plasma mass spectrometry; LCMT, low-coordinate metal target; MC, metal centered; NHC, N-heterocyclic carbene; NMR, nuclear magnetic resonance; OCR, oxygen consumption rate; PDT, photodynamic therapy; PEG, polyethylene glycol; PpIX, protoporphyrin IX; PS, photosensitizer; RPE-1, retinal pigment epithelial cell line; ROS, reactive oxygen species; THF, tetrahydrofuran; U87, human glioblastoma cell line; UV-vis, ultraviolet—visible spectroscopy

REFERENCES

- (1) Karges, J. Clinical Development of Metal Complexes as Photosensitizers for Photodynamic Therapy of Cancer. *Angew. Chem., Int. Ed.* **2022**, *61* (5), No. e202112236.
- (2) Li, X.; Lovell, J. F.; Yoon, J.; Chen, X. Clinical development and potential of photothermal and photodynamic therapies for cancer. *Nat. Rev. Clin. Oncol.* **2020**, *17* (11), 657–674.
- (3) Monro, S.; Colón, K. L.; Yin, H.; Roque, J., 3rd; Konda, P.; Gujar, S.; Thummel, R. P.; Lilge, L.; Cameron, C. G.; McFarland, S. A. Transition Metal Complexes and Photodynamic Therapy from a Tumor-Centered Approach: Challenges, Opportunities, and Highlights from the Development of TLD1433. *Chem. Rev.* **2019**, *119* (2), 797–828.
- (4) Zhang, Y.; Doan, B. T.; Gasser, G. Metal-Based Photosensitizers as Inducers of Regulated Cell Death Mechanisms. *Chem. Rev.* **2023**, 123 (16), 10135–10155.
- (5) Heinemann, F.; Karges, J.; Gasser, G. Critical Overview of the Use of Ru(II) Polypyridyl Complexes as Photosensitizers in One-Photon and Two-Photon Photodynamic Therapy. *Acc. Chem. Res.* **2017**, *50* (11), 2727–2736.
- (6) McKenzie, L. K.; Bryant, H. E.; Weinstein, J. A. Transition metal complexes as photosensitisers in one- and two-photon photodynamic therapy. *Coord. Chem. Rev.* **2019**, *379*, 2–29.
- (7) Zamora, A.; Vigueras, G.; Rodríguez, V.; Santana, M. D.; Ruiz, J. Cyclometalated iridium(III) luminescent complexes in therapy and phototherapy. *Coord. Chem. Rev.* **2018**, *360*, 34–76.
- (8) Zeng, Y.; Liu, L.; Ma, T.; Liu, Y.; Liu, B.; Liu, W.; Shen, Q.; Wu, C.; Mao, Z. Iridium(III) Photosensitizers Induce Simultaneous Pyroptosis and Ferroptosis for Multi-Network Synergistic Tumor Immunotherapy. *Angew. Chem., Int. Ed.* **2024**, *63* (49), No. e202410803.
- (9) Ke, L.; Wei, F.; Xie, L.; Karges, J.; Chen, Y.; Ji, L.; Chao, H. A Biodegradable Iridium(III) Coordination Polymer for Enhanced Two-Photon Photodynamic Therapy Using an Apoptosis-Ferroptosis Hybrid Pathway. *Angew. Chem., Int. Ed.* **2022**, *61* (28), No. e202205429.
- (10) Kuang, S.; Wei, F.; Karges, J.; Ke, L.; Xiong, K.; Liao, X.; Gasser, G.; Ji, L.; Chao, H. Photodecaging of a Mitochondria-Localized Iridium(III) Endoperoxide Complex for Two-Photon Photoactivated Therapy under Hypoxia. *J. Am. Chem. Soc.* **2022**, 144 (9), 4091–4101.
- (11) Abad-Montero, D.; Gandioso, A.; Izquierdo-García, E.; Chumillas, S.; Rovira, A.; Bosch, M.; Jordà-Redondo, M.; Castaño, D.; Bonelli, J.; Novikov, V. V.; Deyà, A.; Hernández, J. L.; Galino, J.; Alberto, M. E.; Francés-Monerris, A.; Nonell, S.; Gasser, G.; Marchán, V. Ruthenium(II) Polypyridyl Complexes Containing COUBPY Ligands as Potent Photosensitizers for the Efficient Phototherapy of Hypoxic Tumors. J. Am. Chem. Soc. 2025, 147 (9), 7360–7376.

- (12) Ellahioui, Y.; Patra, M.; Mari, C.; Kaabi, R.; Karges, J.; Gasser, G.; Gómez-Ruiz, S. Mesoporous silica nanoparticles functionalised with a photoactive ruthenium(ii) complex: exploring the formulation of a metal-based photodynamic therapy photosensitiser. *Dalton Trans.* **2019**, *48* (18), 5940–5951.
- (13) Huang, H.; Yu, B.; Zhang, P.; Huang, J.; Chen, Y.; Gasser, G.; Ji, L.; Chao, H. Highly Charged Ruthenium(II) Polypyridyl Complexes as Lysosome-Localized Photosensitizers for Two-Photon Photodynamic Therapy. *Angew. Chem., Int. Ed.* **2015**, *54* (47), 14049–14052.
- (14) Lu, Y.; Chen, F. Synthesis and Spectroscopic Study of a Homogenous Bimetallic Os(II) Complex as a New Gastric Cancer Photosensitizer. *Chemistry* **2024**, *30* (69), No. e202402861.
- (15) Zhang, P.; Wang, Y.; Qiu, K.; Zhao, Z.; Hu, R.; He, C.; Zhang, Q.; Chao, H. A NIR phosphorescent osmium(ii) complex as a lysosome tracking reagent and photodynamic therapeutic agent. *Chem. Commun.* **2017**, 53 (91), 12341–12344.
- (16) Mani, A.; Feng, T.; Gandioso, A.; Vinck, R.; Notaro, A.; Gourdon, L.; Burckel, P.; Saubaméa, B.; Blacque, O.; Cariou, K.; Belgaied, J.; Chao, H.; Gasser, G. Structurally Simple Osmium(II) Polypyridyl Complexes as Photosensitizers for Photodynamic Therapy in the Near Infrared. *Angew. Chem., Int. Ed.* **2023**, *62* (20), No. e202218347.
- (17) Gourdon, L.; Cariou, K.; Gasser, G. Phototherapeutic anticancer strategies with first-row transition metal complexes: a critical review. *Chem. Soc. Rev.* **2022**, *51* (3), 1167–1195.
- (18) Behm, K.; McIntosh, R. D. Application of Discrete First-Row Transition-Metal Complexes as Photosensitisers. *ChemPlusChem.* **2020**, 85 (12), 2611–2618.
- (19) Roy, M.; Saha, S.; Patra, A. K.; Nethaji, M.; Chakravarty, A. R. Ternary iron (III) complex showing photocleavage of DNA in the photodynamic therapy window. *Inorg. Chem.* **2007**, *46* (11), 4368–4370
- (20) Saha, S.; Majumdar, R.; Roy, M.; Dighe, R. R.; Chakravarty, A. R. An iron complex of dipyridophenazine as a potent photocytotoxic agent in visible light. *Inorg. Chem.* **2009**, *48* (6), 2652–2663.
- (21) Saha, S.; Mallick, D.; Majumdar, R.; Roy, M.; Dighe, R. R.; Jemmis, E. D.; Chakravarty, A. R. Structure— activity relationship of photocytotoxic iron (III) complexes of modified dipyridophenazine ligands. *Inorg. Chem.* **2011**, *50* (7), 2975–2987.
- (22) Basu, U.; Khan, I.; Hussain, A.; Kondaiah, P.; Chakravarty, A. R. Photodynamic Effect in Near-IR Light by a Photocytotoxic Iron (III) Cellular Imaging Agent. *Angew. Chem., Int. Ed.* **2012**, *51* (11), 2658–2661.
- (23) Sahoo, S.; Podder, S.; Garai, A.; Majumdar, S.; Mukherjee, N.; Basu, U.; Nandi, D.; Chakravarty, A. R. Iron (III) Complexes of Vitamin B6 Schiff Base with Boron-Dipyrromethene Pendants for Lysosome-Selective Photocytotoxicity. *Eur. J. Inorg. Chem.* **2018**, 2018 (13), 1522–1532.
- (24) Basu, U.; Khan, I.; Hussain, A.; Gole, B.; Kondaiah, P.; Chakravarty, A. R. Carbohydrate-appended tumor targeting iron (III) complexes showing photocytotoxicity in red light. *Inorg. Chem.* **2014**, 53 (4), 2152–2162.
- (25) Poynton, F. E.; Bright, S. A.; Blasco, S.; Williams, D. C.; Kelly, J. M.; Gunnlaugsson, T. The development of ruthenium (II) polypyridyl complexes and conjugates for in vitro cellular and in vivo applications. *Chem. Soc. Rev.* **2017**, 46 (24), 7706–7756.
- (26) Karges, J.; Goldner, P.; Gasser, G. Synthesis, characterization, and biological evaluation of red-absorbing Fe (II) polypyridine complexes. *Inorganics* **2019**, *7* (1), 4.
- (27) Karges, J.; Gasser, G. Synthesis, Characterisation and Biological Evaluation of π-Extended Fe (II) Bipyridine Complexes as Potential Photosensitizers for Photodynamic Therapy. *Inorg. Chim. Acta* **2020**, 499, No. 119196.
- (28) Behm, K.; McIntosh, R. D. Application of Discrete First-Row Transition-Metal Complexes as Photosensitisers. *ChemPlusChem.* **2020**, 85 (12), 2611–2618.
- (29) Wenger, O. S. Is iron the new ruthenium? *Chem.—Eur. J.* **2019**, 25 (24), 6043–6052.

- (30) Mercs, L.; Albrecht, M. Beyond catalysis: N-heterocyclic carbene complexes as components for medicinal, luminescent, and functional materials applications. *Chem. Soc. Rev.* **2010**, 39 (6), 1903–1912.
- (31) Doddi, A.; Peters, M.; Tamm, M. N-heterocyclic carbene adducts of main group elements and their use as ligands in transition metal chemistry. *Chem. Rev.* **2019**, *119* (12), 6994–7112.
- (32) Kjær, K. S.; Kaul, N.; Prakash, O.; Chábera, P.; Rosemann, N. W.; Honarfar, A.; Gordivska, O.; Fredin, L. A.; Bergquist, K. E.; Häggström, L.; Ericsson, T.; Lindh, L.; Yartsev, A.; Styring, S.; Huang, P.; Uhlig, J.; Bendix, J.; Strand, D.; Sundström, V.; Persson, P.; Lomoth, R.; Wärnmark, K. Luminescence and reactivity of a charge-transfer excited iron complex with nanosecond lifetime. *Science* 2019, 363 (6424), 249–253.
- (33) Estrada-Montaño, A. S.; Ryabov, A. D.; Gries, A.; Gaiddon, C.; Le Lagadec, R. Iron (III) pincer complexes as a strategy for anticancer studies. *Eur. J. Inorg. Chem.* **2017**, *2017* (12), 1673–1678.
- (34) Torres-Gutiérrez, C.; Estrada-Montaño, A. S.; Orvain, C.; Mellitzer, G.; Gaiddon, C.; Le Lagadec, R. Synthesis of Cytotoxic Iron-Containing Macrocycles Through Unexpected C (sp2) C (sp2) Bonds Formation. *Eur. J. Inorg. Chem.* **2023**, 26 (23), No. e202300139.
- (35) Prakash, O.; Lindh, L.; Kaul, N.; Rosemann, N. W.; Losada, I. B.; Johnson, C.; Chábera, P.; Ilic, A.; Schwarz, J.; Gupta, A. K.; Uhlig, J.; Ericsson, T.; Häggström, L.; Huang, P.; Bendix, J.; Strand, D.; Yartsev, A.; Lomoth, R.; Persson, P.; Wärnmark, K. Photophysical Integrity of the Iron (III) Scorpionate Framework in Iron (III)—NHC Complexes with Long-Lived 2LMCT Excited States. *Inorg. Chem.* **2022**, *61* (44), 17515—17526.
- (36) Zisowsky, J.; Koegel, S.; Leyers, S.; Devarakonda, K.; Kassack, M. U.; Osmak, M.; Jaehde, U. Relevance of drug uptake and efflux for cisplatin sensitivity of tumor cells. *Biochem. Pharmacol.* **2007**, *73* (2), 298–307.
- (37) Osellame, L. D.; Blacker, T. S.; Duchen, M. R. Cellular and molecular mechanisms of mitochondrial function. *Best Pract. Res. Clin. Endocrinol. Metab.* **2012**, *26* (6), 711–723.
- (38) Brand, M.; Orr, A.; Perevoshchikova, I.; Quinlan, C. The role of mitochondrial function and cellular bioenergetics in ageing and disease. *Br. J. Dermatol.* **2013**, *169* (s2), 1–8.
- (39) Wallace, D. C. Mitochondria and cancer. *Nat. Rev. Cancer* **2012**, *12* (10), 685–698.
- (40) Agilent Seahorse, X. Glycolysis Stress Test Kit User Guide Kit 103020-100; Agilent Technologies. Inc.: Santa Clara, CA, USA2019.
- (41) Kwong, W.; Lok, C.; Tse, C.; Wong, E. L.; Che, C. Anti-Cancer Iron (II) Complexes of Pentadentate N-Donor Ligands: Cytotoxicity, Transcriptomics Analyses, and Mechanisms of Action. *Chem.—Eur. J.* **2015**, *21* (7), 3062–3072.
- (42) Jungwirth, U.; Kowol, C. R.; Keppler, B. K.; Hartinger, C. G.; Berger, W.; Heffeter, P. Anticancer activity of metal complexes: involvement of redox processes. *Antioxid. Redox Signal.* **2011**, *15* (4), 1085–1127.
- (43) Weiss, D. T.; Anneser, M. R.; Haslinger, S.; Pöthig, A.; Cokoja, M.; Basset, J.-M.; Kühn, F. E. NHC Versus Pyridine: How "Teeth" Change the Redox Behavior of Iron (II) Complexes. *Organometallics* **2015**, *34* (20), 5155–5166.